Available online at www.sciencedirect.com

ScienceDirect

Procedia Structural Integrity 3 (2017) 191–200

Structural Integrity Procedia

www.elsevier.com/locate/procedia

XXIV Italian Group of Fracture Conference, 1-3 March 2017, Urbino, Italy

On the use of the Peak Stress Method for the calculation of Residual Notch Stress Intensity Factors: a preliminary investigation

P. Ferro[a], M. Colussi[a,]*, G. Meneghetti[b], F. Berto[c], M. Lachin[a], S.A. Castiglione[a]

[a]*Department of Engineering and Management, University of Padova, Stradella San Nicola 3, 36100 Vicenza, Italy*
[b]*Department of Industrial Engineering, University of Padova, Via Venezia 1, 35131 Padova, Italy*
[c]*NTNU, Department of Engineering Design and Materials, Richard Birkelands vei 2b, 7491, Trondheim, Norway*

Abstract

Residual stresses induced by welding processes significantly affect the engineering properties of structural components. If the toe region of a butt-welded joint is modeled as a sharp V-notch, the distribution of the residual stresses in that zone is asymptotic with a singularity degree which follows either the linear-elastic or the elastic-plastic solution, depending on aspects such as clamping conditions, welding parameters, material and dimension of plates. The intensity of the local residual stress fields is quantified by the Residual Notch Stress Intensity Factors (R-NSIFs), which can be used in principle to include the residual stress effect in the fatigue assessment of welded joints. Due to the need of extremely refined meshes and to the high computational resources required by non-linear transient analyses, the R-NSIFs have been calculated in literature only by means of 2D models. It is of interest to propose new coarse-mesh-based approaches which allow residual stresses to be calculated with less computational effort. This work is aimed to investigate the level of accuracy of the Peak Stress Method in the R-NSIFs evaluation.

Peer-review under responsibility of the Scientific Committee of IGF Ex-Co.

Keywords: Peak Stress Method; Residual Stress; Finite Element Analysis; Residual Notch Stress Intensity Factor; Sysweld.

1. Introduction

The prediction of failure in components and structures is not just an interesting research topic; it is an essential requirement for our daily live in safety, as pointed out by Miller (2003). There are many ways in which failures

* Corresponding author. Tel.: +39 0444 998711; fax: +39 0444 998888.
E-mail address: marco.colussi.1@phd.unipd.it

Peer-review under responsibility of the Scientific Committee of IGF Ex-Co.
10.1016/j.prostr.2017.04.037

occur: brittle fracture, plastic collapse, buckling and fatigue, to mention a few. The external loads acting on a component are usually considered because clearly important, but other factors often play a determining role: pre-existing microstructural features or defects and residual stresses, especially in large scale components, as shown by Launert et al. (2017). Compared with the role of defects, the role of residual stresses on failure usually receives less attention, probably because of the difficulties associated with their evaluation and measurement, hindered by the fact that they do not produce visible effects, as explained by Withers (2007).

Nomenclature

d	adopted finite element size
r,θ	cylindrical coordinates
K_1	mode 1 Stress Intensity Factor (SIF)
K_1	mode 1 Notch Stress Intensity Factor (NSIF)
σ_r, σ_θ	stress components in a cylindrical frame of reference
σ_{peak}	linear elastic peak stress calculated by FEM at the sharp V-notch tip by means of a given mesh pattern
2α	opening angle of the V-shaped notch
λ_1	first Williams' eigenvalue
L	butt-joint width
h	butt-joint thickness
q	power density of the heating source
Q^*	power input
η	efficiency
Q	absorbed power
a, b	molten pool dimensions
c_1, c_2	molten pool dimensions
f_1, f_2	constants for the energy distribution of the heat flux
τ	time at which the heat flux is maximum
t	actual time of welding simulation
v	welding speed

Depending on the sign (tensile or compressive), residual stresses are added to, or subtracted from, in-service stresses. As a consequence, unexpected failures often occur because residual stresses have critically combined with in-service stresses, or because they have lowered the stress at which failure occurs in the presence of undetected defects. Moreover, residual stresses due to welding processes could significantly affect high cycle fatigue (HCF) life of welded joints: tensile residual stresses have unfavorable effects on HCF, whereas in the presence of compressive residual stresses the fatigue resistance is improved, which can be interpreted in terms of crack closure phenomenon as shown by Beghini et al. (1994), by Bertini et al. (1998) and by Yung and Lawrence (2013). Phase transformation effects (both volume change and transformation plasticity) have a great influence on the intensity and sign of the local stress fields near the weld toe region, as proved by Ferro (2012): according to the joint geometry and both the dimension and the shape of the Heat Affected Zone (HAZ), the phase transformation effects may change the sign of the local residual stress fields. Therefore, in structural integrity terms it is important to know if residual stresses are tensile or compressive and to include them into structural assessments so that corrective reparative action can be carried out when necessary.

In welded joints subjected to fatigue loading, cracks systematically initiate and propagate from the weld toe or the weld root, where high stress concentration effects are present. If the weld toe region is modeled as a sharp V-shaped notch (zero radius), the stress distribution in the proximity of this zone is linear in a log–log scale and its slope corresponds to the analytical solution provided by Williams (1952). According to Lazzarin and Tovo (1998), the intensity of such stress distribution is quantified through the so-called Notch Stress Intensity Factors (NSIFs). A relatively recent contribution by Ferro et al. (2006) in this direction demonstrated that ahead of sharp V-notches the thermal stresses induced by a steady thermal load have the same asymptotic nature of the stress fields induced by

mechanical loads. Therefore, new thermal-load-induced NSIFs have been defined as the natural extension of those related to external mechanical loads. Residual stress distributions in butt-welded joints near the weld toe are singular in the context of the NSIF approach; in this case, the notch stress intensity factors can be properly expressed as Residual Notch Stress Intensity Factors (R-NSIFs) as shown by Ferro et al. (2006) and by Ferro and Petrone (2009). In literature the R-NSIFs have been used by Ferro (2014) to quantify the influence of residual stresses on high cycle fatigue life of butt-welded joints, where no stress redistribution due to local plasticity phenomena is expected to be present. However, since extremely refined meshes are needed and high computational resources are required by the transient and non-linear welding process simulation, R-NSIFs are usually calculated by means of 2D models under generalized plain strain conditions.

Nisitani and Teranishi (2001 and 2004) showed that the linear elastic stress σ_{peak}, calculated at a crack tip through a Finite Element (FE) model characterized by a mesh pattern having a constant element size, can be used to estimate the value of the mode 1 Stress Intensity Factor (K_1) for a crack initiating from an elliptical hole. In particular, they demonstrated that the K_1 to σ_{peak} ratio depends only on the finite elements size and does not depend on the crack size. Then the σ_{peak} value can be used to rapidly estimate the K_1 value, assuming that both the mesh pattern and the finite element type have been previously calibrated on geometries for which the exact value of K_1 is known. Meneghetti and Lazzarin (2007) provided a theoretical justification to this approach, which has been called Peak Stress Method (PSM). Thereafter, for the purpose of having a rapid fatigue assessment of fillet welded joints, the PSM has been calibrated for weld-like geometries and analytical expressions have been derived for the NSIFs estimation at the weld toe and the weld root, assumed that both points of singularity are modeled as sharp V-notches, as shown by Meneghetti (2008) and Meneghetti and Lazzarin (2011).

The aim of this work is to investigate the level of accuracy of the Peak Stress Method in the rapid estimation of R-NSIFs induced by thermal loads near a V-notch tip. With this purpose, the weld toe region of a butt-welded joint has been considered and residual stress fields have been determined by means of a dedicated FE code, Sysweld®. Different materials (which experience and do not experience phase transformations during thermal cycles), different heat source power, mesh size and joint dimensions have been considered to give general meaning to the investigation. The possibility of quantifying the degree of singularity and the intensity of the residual stress distribution near a weld toe by means of a rapid evaluation of R-NSIFs might be of great interest, particularly in three-dimensional cases.

2. The Peak Stress Method analytical frame

Under the assumption of linear-elastic plane-stress or plane-strain conditions, the analytical expression for the stress field near a sharp V-notch tip has been given by Williams (1952), for both mode 1 and mode 2 loading condition.

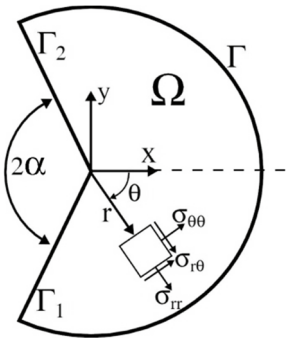

Fig. 1. Domain Ω for the sharp V-notch problem according to Williams' analytical frame.

By using only the first term of the Williams' expansion series in mode 1 loading condition (opening condition) for the V-notch, the stress field around the tip (Fig. 1) can be described by the following equation:

$$\sigma_{ij}(r,\theta) = \frac{K_1}{r^{1-\lambda_1}} f_{ij}^1(\theta) \qquad (i,j = r,\theta) \tag{1}$$

where $f_{ij}^1(\theta)$ are angular functions whose closed form expressions have been provided by Livieri and Lazzarin (2005), λ_1 is the first eigenvalue defined by the expression:

$$\lambda_1 \sin(q\pi) + \sin(q\pi\lambda_1) = 0 \tag{2}$$

where $q=(2\pi-2\alpha)/\pi$ and K_1 is the NSIF which quantifies the intensity of the local stress field according to Gross and Mendelson (1972):

$$K_1 = \sqrt{2\pi} \lim_{r\to 0} r^{1-\lambda_1} \sigma_{\theta\theta}(r,\theta=0) \tag{3}$$

The first eigenvalue depends only on the V-notch opening angle (2α) and varies in a range between 0.5 (when 2α=0) and 0.757 (when 2α=5π/6) so that Eq. (1) contains a singular term (r^{λ_1-1} when r→0).

According to the PSM, there exists an analytical expression which estimate the ratio K^*_{FE} linking the NSIF for a sharp V-notch and the linear elastic peak stress obtained from FE analyses at the point of singularity of the same geometrical feature:

$$K^*_{FE} = \frac{K_1}{\sigma_{peak} \cdot d^{1-\lambda_1}} \tag{4}$$

where K_1 is the exact mode 1 NSIF of the analyzed geometry and σ_{peak} is the linear elastic peak stress, as calculated with the FE method by using a pattern of elements having constant finite element size d.

The conditions under which Eq. (4) is valid are: a) the pattern of FEs around the toe of a welded joint must be as close as possible to the one which is shown in Fig. 2, i.e. two FEs must share the node located at the singular point; b) notch opening angle ranging from 0 to 135°. When the previous conditions are satisfied, Eq. (4) states that, once fixed the finite element size, the ratio of K_1 over σ_{peak} is constant. Then the NSIF K_1 can be estimated by means of the elastic peak stress σ_{peak}.

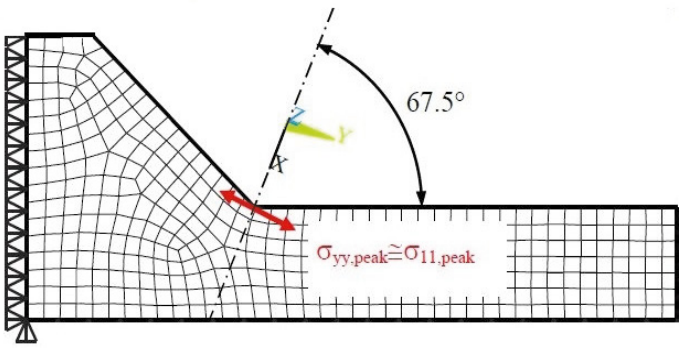

Fig. 2. Typical welded joint geometry and mesh pattern according to the PSM.

3. Finite element model

A butt-welded joint has been analyzed using the finite element code Sysweld®, under generalized plane strain hypothesis. The jointed plates have variable width (L) and fixed thickness (h) equal to 6 mm (Fig. 3). The weld toe has been modeled as a sharp, zero radius, V-shaped notch with an opening angle (2α) equal to 135°. Two different materials have been considered: a carbon steel with chemical composition according to the Standard ASTM SA 516 (Grade 65 resp. 70) and an Al alloy AA 5083. Thermo-mechanical properties of the base material have been taken from Sysweld® database. Room temperature thermal properties have been employed, because it is known from literature that temperature and residual stress distributions are slightly affected by thermal properties' dependence on temperature as proved by Zhu and Chao (2002), Barroso et al. (2010) and Bhatti and al. (2015). On the other hand, residual stress distributions are strongly dependent on the variation of the mechanical properties with temperature, thus the yield stress range has been taken into account.

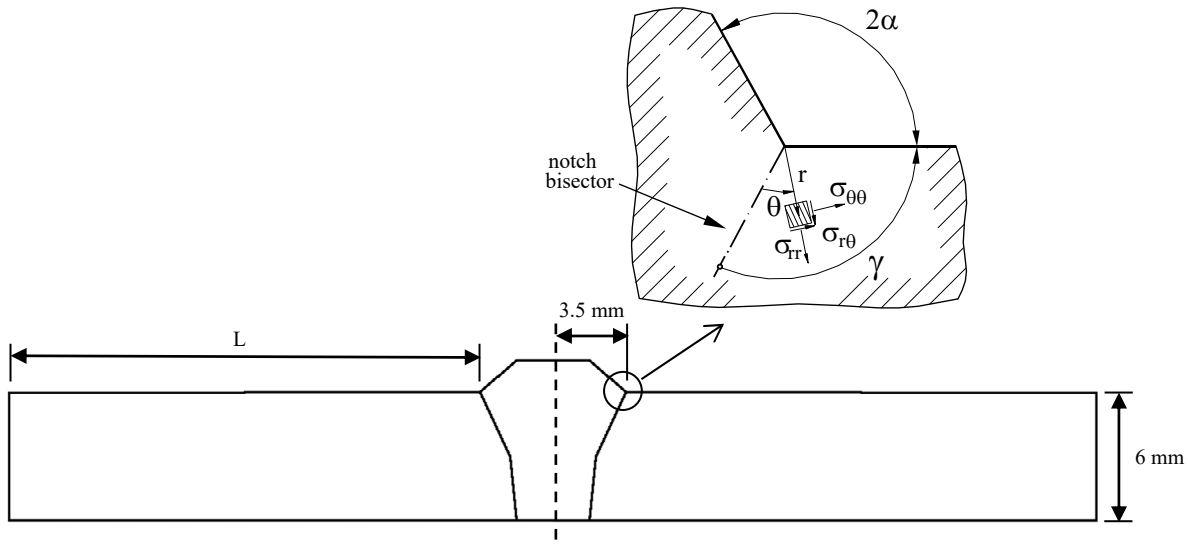

Fig. 3. Schematic representation of the butt-welded joint considered in the present work and the polar coordinate system centered at the V-notch tip.

Radiative (using the Stephan-Boltzman law) and convective heat loss (using a convective heat transfer coefficient equal to 25 W/m^{2}K) have been applied at the boundary (external surfaces) of the plates to be joined. For the analyzed steel, thermo-metallurgical and mechanical properties as a function phase and temperature have been taken into account [Sysweld Toolbox 2011®]. In the metallurgical analysis the following phases have been included: martensite, bainite, ferrite-pearlite. The metallurgical transformations mainly depend on thermal history, with this dependence described by Continuous Cooling Transformation (CCT) diagrams, which plot the start and the end transformation temperatures as a function of cooling rate or cooling time. In the present work the diffusion-controlled phase transformations and the displacive martensitic transformation have been modeled according to Leblond and Devaux (1984) and to Koistinen and Marburger (1959) by means of the Leblond-Devaux kinetic law, respectively. Fig. 4 shows the CCT diagrams that have been implemented in the model.

The thermal energy flow into the material during the welding process represents the only computational load modeled in the welding simulation. The amount of thermal energy flow into the material is determined by the welding parameters (including welding speed) and by the welding technology used. In this work the heat source has been modeled using a double ellipsoid power density distribution function given by Goldak et al. (1984) and described by (Eq. 5), which has been widely used in literature for arc welding simulation, see for instance Ferro et al. (2010).

$$q(x,y,t)=\frac{6\sqrt{3}\,f_{1,2}\,Q}{\pi\sqrt{\pi}\,a\,b\,c_{1,2}}e^{-\frac{3x^2}{a^2}}e^{-\frac{3y^2}{b^2}}e^{-\frac{3[v(\tau-t)]^2}{c_{1,2}^2}} \tag{5}$$

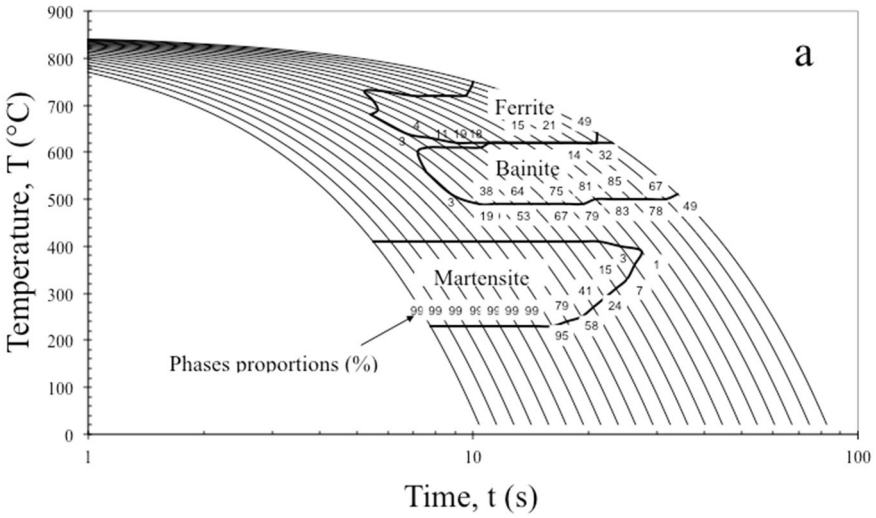

Fig. 4. CCT diagrams of the steel under investigation.

The double ellipsoid heat source and the meaning of the symbols used in Eq. (5) are shown in Fig. 5, whereas the adopted numerical values are summarized in Table 1.

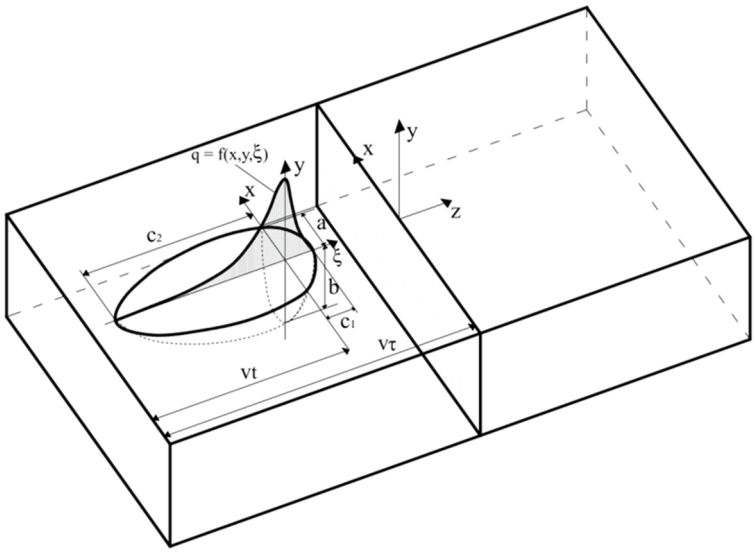

Fig. 5. Double ellipsoid heat source configuration together with the power distribution function along the ξ axis of the moving coordinate system (x,y,ξ). The transformation relating the fixed and the moving coordinate system is $\xi = z + v(\tau - t)$.

By taking advantage of the double symmetry, one half of the joint has been modeled. In Fig. 6 the mesh patterns used in the calculation of R-NSIFs from local stress fields (Fig. 6.a) and the ones used for the PSM evaluation (Fig. 6.b) are compared, respectively.

Table 1. Goldak's source parameters (used for the Al alloy).

q	Power density [W/m^3]	see Eq. 5
Q^*	Power input [W]	see Table 2
η	Efficiency	0.64
Q	Absorbed power [W]	$\eta \cdot Q^*$
a	Molten pool dimensions [mm]	3.5
b		11
c_1		2.3
c_2		7.9
f_1	Fractions of the heat deposit in the front and rear quadrants, with $f_1+f_2=2$	0.6
f_2	(subscript 1 for $\xi > 0$; subscript 2 for $\xi < 0$)	1.4
v	Welding speed [mm/s]	11
τ	Total time spent by the welding source to be over the transverse cross section of the plate [s]	3

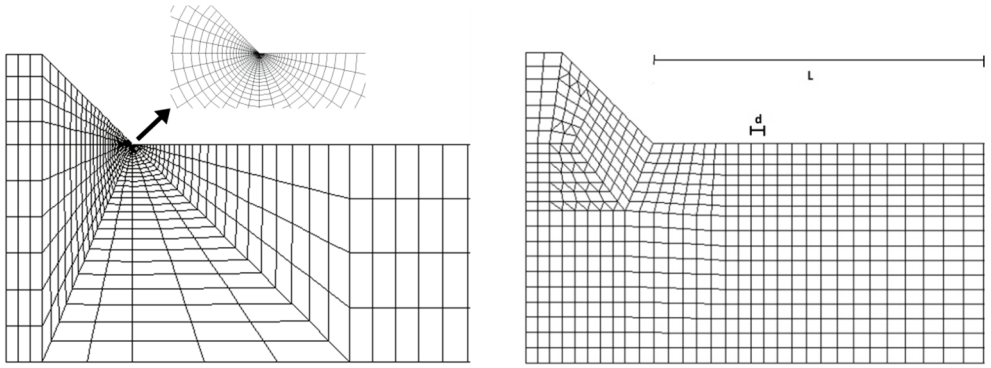

(a) (b)

Fig. 6. Finite element model: (a) very fine pattern used to compute R-NSIFs from local stress fields and detail of the notch tip refinement (order of magnitude of the smallest element equal to 10^{-4} mm); (b) coarse pattern with constant element size d according to the PSM (order of magnitude of the smallest element equal to 10^{-1} mm);.

The FE model used to compute R-NSIFs from local stress fields was defined by approximately 2700 linear isoparametric elements. At the notch tip, the minimum size of the elements was about $5 \cdot 10^{-4}$ mm, according to Lazzarin and Tovo (1998). The FE model used to estimate R-NSIFs by means of the PSM was defined by approximately 700 linear isoparametric elements. The mesh pattern was characterized by two elements sharing the node located at the weld toe and by an element size d (defined in Table 2) kept as constant as possible in the whole model, according to Meneghetti and Lazzarin (2007). Finally, uncoupled thermo-mechanical analyses have been carried out. The molten effect has been simulated by using a function that clears the history of an element whose temperature exceeds the melting temperature. All the analyses have been performed on a MacBook Pro provided with a Intel Core i7 2.6 GHz processor (4 core) and 16 GB of RAM.

4. Results and discussion

The asymptotic nature of the residual stress distribution near a sharp V-notch has been numerically investigated in the present paper. With this purpose, a simple geometry with a sharp V-notch tip has been considered under

generalized plane hypothesis: the weld toe region of a butt-welded joint. Thermo-mechanical, uncoupled, finite element transient simulations of the welding process have been carried out in Sysweld® environment. Two materials, which present and do not present phase transformation, i.e. a carbon steel and an Al alloy, have been considered and the arc welding torch has been modeled by means of Goldak's source.

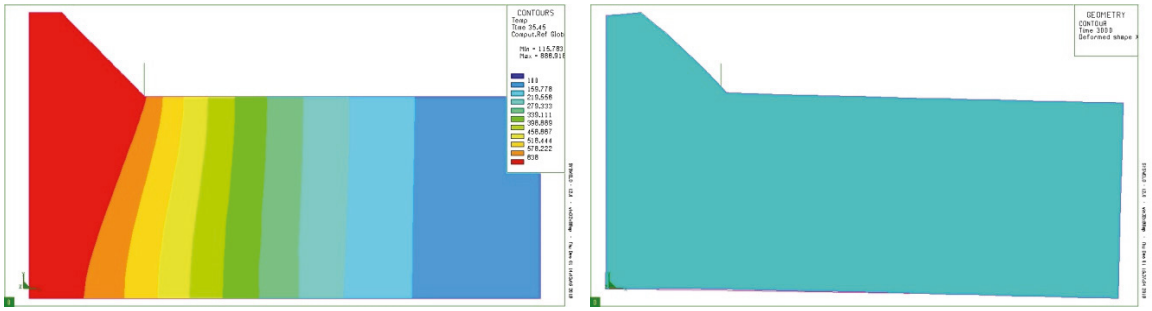

(a) (b)

Fig. 7. (a) Temperature distribution at the instant of maximum width of the fusion zone (in red); (b) deformed shape at the end of the simulation.

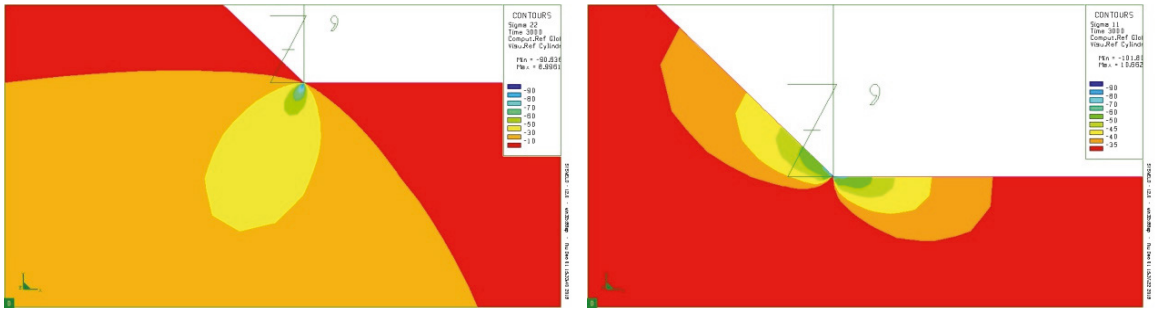

(a) (b)

Fig. 8. Residual stress distribution near the notch tip: (a) $\sigma_{\theta\theta}$ component of stress; (b) σ_{rr} component of stress.

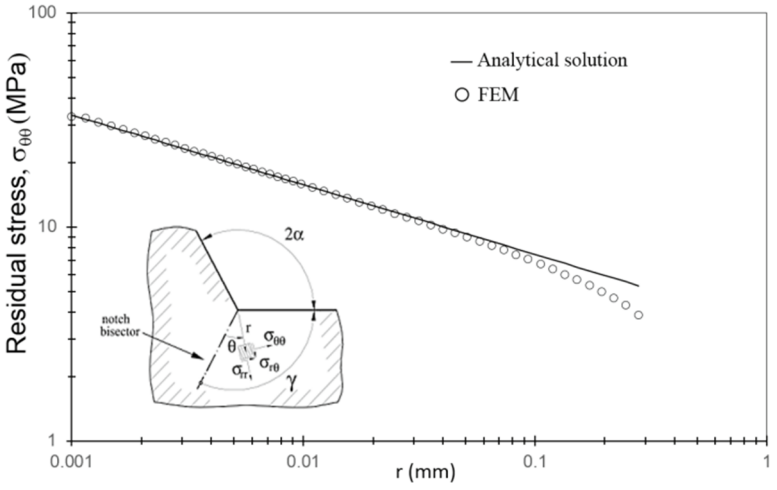

Fig. 9. Asymptotic $\sigma_{\theta\theta}$ component of the residual stress field near the notch tip along the plane bisecting the notch angle, i.e. θ=0°.

Fig. 7.a shows the qualitative temperature distribution when the melted zone has reached its maximum extension. The corresponding residual deformed shape at the end of the cooling process, shown in Fig. 7.b, is in perfect

agreement with the one experimentally obtained in similar cases. The stress field distributions near the toe region are reported in Fig. 8, according to a cylindrical coordinate system centered at the notch tip: Fig. 8.a and 8.b show $\sigma_{\theta\theta}$ and σ_{rr} stress components, respectively. The stress distribution near the weld toe is linear in a log-log plot (Fig. 9) and its slope corresponds to the analytical solution given by Eq. (1). The intensity of such residual stress field has therefore been given in terms of R-NSIFs.

In Table 2 the obtained results are summarized. Regardless of whether or not the material experiences a phase transformation (i.e. carbon steel and Al alloy), the mesh size, the source power and the joint length, it is possible to notice a good agreement between the K_1 values obtained from the local stress field computed with very fine meshes and the ones estimated by means of the PSM and coarse meshes, if a constant value of about 1.71 for K^*_{FE} is used. The outcome of this preliminary investigation is that the PSM seems suitable for a rapid R-NSIF evaluation, leading to a remarkable reduction of the computational costs associated with the residual stress estimation in welded joints. To apprise the computational advantage associated to the use of the PSM, the solution times are reported in the following. The solution time associated to the very refined meshes was about 01':07" for thermal analyses and 03':50" for mechanical analyses, whereas the one associated to the PSM mesh pattern was about 00':10" for thermal analyses and 00':52" for mechanical analyses.

In conclusion, the following main advantages can be outlined if the R-NSIFs are estimated by means of the PSM rather than directly computed from local stress fields: (i) only one nodal stress value calculated at the point of singularity is sufficient to compute the R-NSIF, the whole stress distribution along the notch bisector being no longer required; (ii) three orders of magnitude more coarse meshes could be employed by using the PSM compared to the very refined meshes required to evaluate the local stress field directly. In the authors' opinion, both reasons make the PSM of easy and fast applicability in industrial and research applications. The PSM appears also suitable for residual stress evaluations by means of three-dimensional FE models.

Table 2. Comparison between the values of the R-NSIFs evaluated with very fine meshes and coarse meshes, both using linear isoparametric elements, taking advantage of Eq. (4) linking the peak stress and the mode 1 R-NSIF. Variable geometrical parameters are defined in Fig. 3 and in Fig. 6.

Materials	Q^* (W)	L (mm)	d (mm)	Fine mesh K_1 (MPa mm$^{0.326}$)	Coarse PSM mesh		
					σ_{peak} (MPa)	K_1 (MPa mm$^{0.326}$)	Δ%
Steel	10500	12	0.286	71.0	62.7	71.3	0.4
Steel	10500	100	0.286	81.0	71.3	81.1	0.1
Steel	11500	12	0.286	42.0	35.5	40.4	-3.9
Al alloy	2400	12	0.286	46.0	40.6	46.2	0.4
Al alloy	2900	12	0.286	43.0	37.7	42.9	-0.2
Al alloy	2900	100	0.286	8.8	7.8	8.9	1.1
Al alloy	2900	100	0.143	8.8	10.2	9.3	5.7

5. Conclusion

The suitability of the PSM in the R-NSIF evaluation has been investigated. Given a butt weld geometry, modeled as a sharp V-notch with a 135° opening angle, a set of local residual stress distributions have been obtained by means of the dedicated FE code Sysweld®, under generalized plane strain hypothesis. Different materials, source power, joint dimensions and mesh size have been considered and it has been found that the ratio between the R-NSIF and the peak stress value is constant for a given mesh pattern. The PSM appears therefore suitable for a rapid, coarse mesh based, R-NSIF evaluation. Further advantage of the PSM is that it combines the robustness of the stress field based methods (like the NSIF approach) with the simplicity of the point-stress related methods.

References

Barroso, A., Cañas, J., Picón, R., París, F., Méndez, C., Unanue, I., 2010. Prediction of welding residual stresses and displacements by simplified models. Experimental validation. Materials and Design 31, 1338–1349.

Beghini, M., Bertini, L., Vitale, E., 1994. Fatigue residual stress fields. Experimental results and modelling. Fatigue and Fracture of Engineering Materials and Structures 17, 1433–1444.

Bertini, L., Fontanari, V., Straffelini, G., 1998. Influence of post weld treatments on the fatigue behaviour of Al-alloy welded joints. Science 20, 749–755.

Bhatti, A.A., Barsoum, Z., Murakawa, H., Barsoum, I., 2015. Influence of thermo-mechanical material properties of different steel grades on welding residual stresses and angular distortion. Materials and Design 65, 878–889.

Ferro, P., 2012. Influence of phase transformations on the asymptotic residual stress distribution arising near a sharp V-notch tip. Modelling and Simulation in Materials Science and Engineering 20, 085003.

Ferro, P., 2014. The local strain energy density approach applied to pre-stressed components subjected to cyclic load. Fatigue and Fracture of Engineering Materials and Structures 37, 1268–1280.

Ferro, P., Berto, F., Lazzarin, P., 2006. Generalized stress intensity factors due to steady and transient thermal loads with applications to welded joints. Fatigue and Fracture of Engineering Materials and Structures 29, 440–453.

Ferro, P., Petrone, N., 2009. Asymptotic thermal and residual stress distributions due to transient thermal loads. Fatigue and Fracture of Engineering Materials and Structures 32, 936–948.

Ferro, P., Bonollo, F., Tiziani, A., 2010. Methodologies and experimental validations of welding process numerical simulation. International Journal of Computational Materials 3, 114–132.

Goldak, J., Chakravarti, A., Bibby, M., 1984. A new finite element model for welding heat sources. Metallurgical Transactions B 15, 299–305.

Gross, B., Mendelson, A., 1972. Plane elastostatic analysis of V-notched plates. International Journal of Fracture Mechanics 8, 267–276.

Koistinen, D.P., Marburger, R.E., 1959. A general equation prescribing extent of austenite-martensite transformation in pure iron-carbon alloys and carbon steels. Acta Metallurgica 7, 59–68.

Launert, B., Rhode, M., Kromm, A., Pasternak, H., Kannengiesser, T., 2017. Measurement and numerical modeling of residual stresses in welded HSLA component-like I-girders. Welding in the World 61, 223–229.

Lazzarin, P., Tovo, R., 1998. A Notch Intensity Factor Approach To the Stress Analysis of Welds. Fatigue and Fracture of Engineering Materials and Structures 21, 1089–1103.

Leblond, J.B., Devaux, J., 1984. A new kinetic model for anisothermal metallurgical transformations in steels including effect of austenite grain size. Acta Metallurgica 32, 137–146.

Livieri, P., Lazzarin, P., 2005. Fatigue strength of steel and aluminium welded joints based on generalised stress intensity factors and local strain energy values. International Journal of Fracture 133, 247–276.

Meneghetti, G., Lazzarin, P., 2007. Significance of the elastic peak stress evaluated by FE analyses at the point of singularity of sharp V-notched components. Fatigue and Fracture of Engineering Materials and Structures 30, 95–106.

Meneghetti, G., Lazzarin, P., 2011. The Peak Stress Method for Fatigue Strength Assessment of welded joints with weld toe or weld root failures. Welding in the World 55, 22–29.

Meneghetti, G., 2008. The peak stress method applied to fatigue assessments of steel and aluminium fillet-welded joints subjected to mode I loading. Fatigue and Fracture of Engineering Materials and Structures. 31, 346–369.

Miller, K.J., 2003. Structural integrity — whose responsibility? Proceedings of the I MECH E Part L Journal of Materials,Design and Applications 217, 1–21.

Nisitani, H., Teranishi, T., 2004. KI of a circumferential crack emanating from an ellipsoidal cavity obtained by the crack tip stress method in FEM. Engineering Fracture Mechanics 71, 579–585.

Williams, M.L., 1952. Stress singularities resulting from various boundary conditions in angular corners of plates in extension. Journal of Applied Mechanics 19, 526–528.

Withers, P.J., 2007. Residual stress and its role in failure. Reports on Progress in Physics 70, 2211–2264.

Yung, J., Lawrence, F., 2013. Predicting the fatigue life of welds under combined bending and torsion. ICBMFF2.

Zhu, X.K., Chao, Y.J., 2002. Effects of temperature-dependent material properties on welding simulation. Computers and Structures 80, 967–976.